

Molecular Physics

An International Journal at the Interface Between Chemistry and Physics

ISSN: 0026-8976 (Print) 1362-3028 (Online) Journal homepage: <http://www.tandfonline.com/loi/tmph20>

Theoretical study on structural and electronic properties of solid anthracene under high pressure by density functional theory

Ling-Ping Xiao, Guo-Hua Zhong, Zhi Zeng & Xiao-Jia Chen

To cite this article: Ling-Ping Xiao, Guo-Hua Zhong, Zhi Zeng & Xiao-Jia Chen (2016) Theoretical study on structural and electronic properties of solid anthracene under high pressure by density functional theory, *Molecular Physics*, 114:2, 283-289, DOI: [10.1080/00268976.2015.1099753](https://doi.org/10.1080/00268976.2015.1099753)

To link to this article: <http://dx.doi.org/10.1080/00268976.2015.1099753>



Published online: 26 Oct 2015.



Submit your article to this journal [↗](#)



Article views: 65



View related articles [↗](#)



View Crossmark data [↗](#)

RESEARCH ARTICLE

Theoretical study on structural and electronic properties of solid anthracene under high pressure by density functional theory

HPSTAR
2016-258

Ling-Ping Xiao^{a,b}, Guo-Hua Zhong^c, Zhi Zeng^{a,b} and Xiao-Jia Chen^{a,d}

^aKey Laboratory of Materials Physics, Institute of Solid State Physics, Chinese Academy of Sciences, Hefei, China; ^bUniversity of Science and Technology of China, Hefei, China; ^cShenzhen Institutes of Advanced Technology, Chinese Academy of Sciences, Shenzhen, China; ^dCenter for High Pressure Science and Technology Advanced Research, Shanghai, China

ABSTRACT

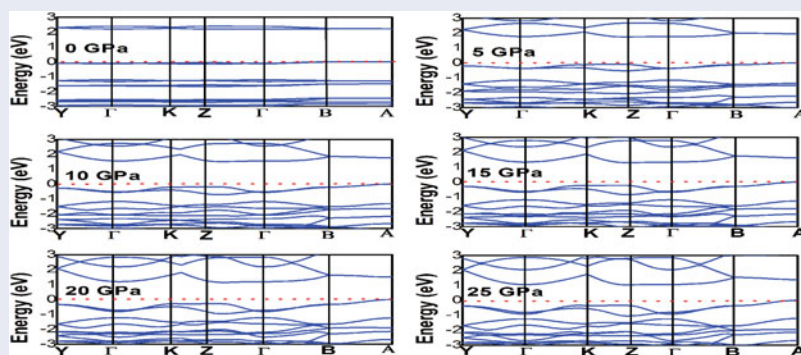
Based on the density functional theory, a theoretical determination method is applied to investigate structural and electronic properties of anthracene up to 27 GPa. The lattice parameters a , b , c , decrease by 1.53 Å (−18.2%), 0.76 Å (−12.8%), and 0.93 Å (−8.4%), respectively, while the monoclinic angle β increased by 4.65° in this pressure region. At the highest pressure of 27 GPa the unit cell volume is decreased by 58.9%. These findings are shown to be in agreement with experimental results and hint towards the evolution of intermolecular interaction with pressure. The calculated electronic band splitting and the band gap reduce smoothly to some extent with the pressure increasing. Moreover, a pressure-induced decrease of the band gap is observed.

ARTICLE HISTORY

Received 5 May 2015
Accepted 21 September 2015

KEYWORDS

Aromatic hydrocarbons;
density functional
calculations; high pressure



1. Introduction

Molecular crystals – built of π conjugated molecules – have attracted considerable attention, as these systems seem to be promising candidates for low-cost, easy processable materials for electro-optical and electronic applications [1–4]. Anthracene as a representative of the large class of polycyclic aromatic hydrocarbons (PAHs) have served for a long time as model compounds for organic molecular crystals. Due to the relatively weak intermolecular interaction of PAHs, the characteristic of these solids is very responsive to applied pressure [5]. In some cases, this has resulted in intriguing and unexpected physical properties, such as metallic behaviour [6] and superconductivity [7,8].

Pure anthracene molecule consists of three benzene rings arranged in a herringbone manner similar to naphthalene which is the first member in the series of fused

polyaromatic molecules [9]. The crystal structure of solid anthracene is shown in Figure 1. The main feature of the arrangement of the anthracene molecule is that the long molecular axes of the two translationally inequivalent molecules are tilted to each other. Crystal structure, molecular packing, and relative molecular orientation in a molecular crystal can be altered by change in temperature, pressure, electric and magnetic fields [10]. Temperature-dependent single crystal studies revealed some changes in the molecular packing of anthracene and weak changes in the conformation of the individual molecules [11]. The pressure effect on the crystal structure of anthracene has been discussed earlier in terms of the cell parameters and packing angles [12,13]. Many experimental and theoretical investigations have been carried out for anthracene as a function of pressure. Oehzelt et al. have reported the crystalline

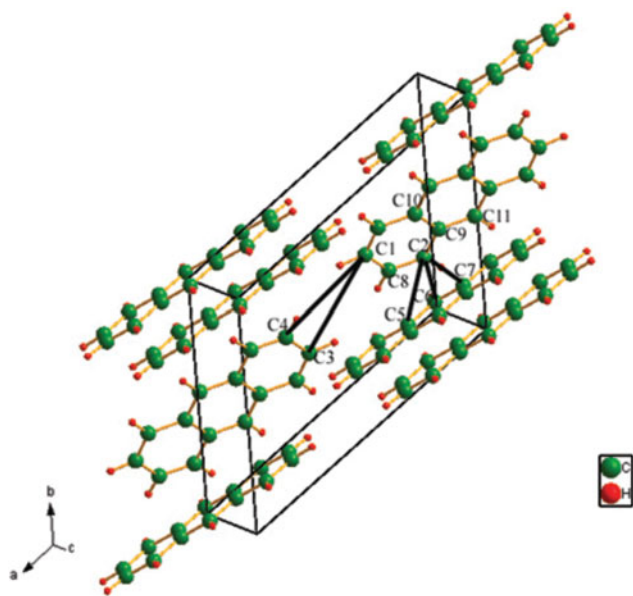


Figure 1. Crystal structure of anthracene.

structure information of anthracene under high pressure up to 10.2 GPa by using angle dispersive X-ray diffraction experiments [14]. Dreger et al. report pressure-induced changes on the fluorescence spectra up to 5 GPa [15]. Recently, Resel et al. provided the crystallographic structure changes of anthracene under hydrostatic and non-hydrostatic pressure conditions up to 27 GPa [16]. These experiments report that under hydrostatic conditions there is no evidence of a structural phase transition up to 27 GPa at room temperature. Meanwhile, first-principles calculations on anthracene revealed the unique electronic and optical properties in this organic compound [17]. Tkatchenko and colleagues established that in some cases the inclusion of many-body van der Waals (vdW) interactions may play a substantial role in the properties of molecular crystals [18–20]. Taking into consideration, these interactions systematically improves the agreement between the calculated and experimental values of sublimation enthalpy of molecular crystals [21]. The isothermal bulk moduli, electronic band structures, and dielectric tensors as a function of the unit cell volume up to 10.5 GPa have been reported by Hummer et al. [22]. High pressure results in the tuning of electronic and structural properties in the materials that are useful to extract the relationships between the structure and electronic, optical, magnetic properties. Here, we provide a clear picture about pressure dependence of anthracene crystal structure and electronic band structure up to 27 GPa. The calculations were carried out up to 27 GPa due to the availability of rich experimental results on the crystal structure and packing of molecules and a direct comparison of our results can be made with the experimental results. In

this paper, the information of the pressure dependence of lattice parameters, the electronic band structure, and the energy gap are provided.

2. Computational details

The calculations carried out in this work are based on the density functional theory (DFT) using the CASTEP program package [23]. The GGA functional of Perdew–Burke–Ernzerhof (PBE) was employed [24]. Pervasive vdW interaction contributions, which are common in molecular crystals, were added using the Tkatchenko and Scheffler (TS) method [25]. The valence pseudowave functions were expanded in a plane-wave basis set with a cut-off energy of 750 eV. The full geometries (lattice parameters for crystals and coordinates for both crystals and molecules) were optimised at the PBE+TS level, with convergence criteria of 5×10^{-6} eV/atom for total energy, 0.01 eV/Å for max force, 0.02 GPa for max stress, and 5×10^{-4} Å for max displacement. The Vanderbilt ultra-soft pseudopotentials and Broyden–Fletcher–Goldfarb–Shanno (BFGS) algorithm were used in our calculations [26]. The used potentials in our calculations are H-00PBE and C-00PBE.

We first build the crystal of anthracene in the monoclinic space group $P2_1/a$ with experimental lattice constants of $a = 8.554$ Å, $b = 6.016$ Å, $c = 11.174$ Å, and $\beta = 124.60^\circ$ [9]. The external pressure was gradually increased by an increment of 1 GPa. The structure at each pressure was geometry optimised using the BFGS and minimised within CASTEP, which uses a starting Hessian that is recursively updated during optimisation. In accordance with the work of Kovalev, the high-symmetry points in units of $(2\pi/a, 2\pi/b, 2\pi/c)$ are carried out following a path along $Y = (0.5, 0, 0)$, $\Gamma = (0, 0, 0)$, $K = (0.4, 0, 0.2)$, $Z = (0, 0, 0.5)$, $B = (0, 0.5, 0)$, and $A = (0.5, 0.5, 0)$, respectively [22].

3. Results and discussion

3.1. Internal geometry

Pristine anthracene is a typical kind of molecular solid and each unit cell contains two molecules. In order to test the reliability of the optimised geometries, we have calculated the average difference in absolute value between the experimental and calculated lattice parameters reported in Table 1. The overall deviations between our calculations and the experiments are less than 2% in lattice parameters and unit cell volumes. After lattice parameters and inner atom positions relaxation, we obtain the lattice parameters of pristine anthracene, $a = 8.399$,

Table 1. Calculated and experimental structural data of the crystal anthracene under zero pressure.

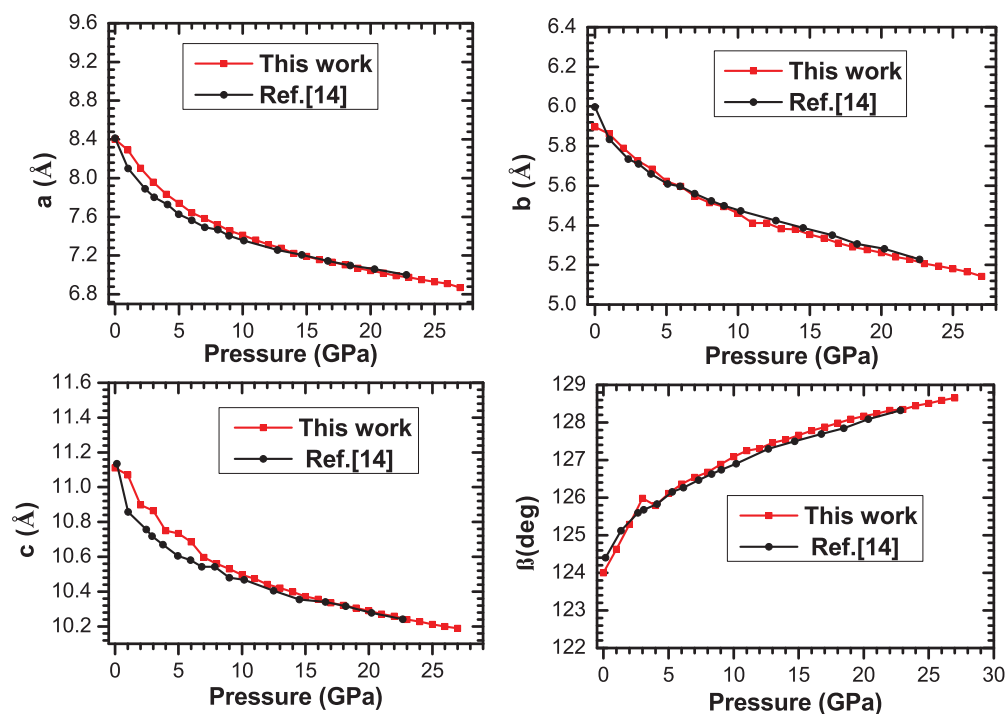
Structure	Other work [33]	Expt.(92 K) [9]	GGA	PBE + vdW
a_0 (Å)	8.562	8.554	9.507	8.399
b_0 (Å)	6.038	6.016	6.356	5.906
c_0 (Å)	11.184	11.172	11.495	11.112
β (°)	124.7°	124.6°	122.89°	124.7

$b = 5.906$, $c = 11.120$, and $\beta = 124^\circ$, in a perfect agreement with the experimental parameters, $a = 8.414$, $b = 5.990$, $c = 11.095$, and $\beta = 124^\circ$, together with the available experimental data and other theoretical results for comparison [14]. Our GGA calculations overestimate a , b , and c by 11.2%, 5.6%, and 2.9%, respectively. Such discrepancy between theory and experiment is mainly due to a lack of vdW dispersion force in the DFT-GGA functional used. When using PBE + vdW method to model the crystalline structures of these oligoacene crystals, the unit cell parameters are in excellent agreement with the experimental values. These results point out that the PBE + vdW method yields better lattice parameters values for this type of aromatic hydrocarbons than the GGA method.

Pressure is a well-suited parameter for producing large changes in intermolecular interactions and crystal structure. Pressure dependence of the lattice parameters a ,

b , c , and β of our work are showed in Figure 2. As expected, the lattice parameters a , b , and c decrease with increasing pressure. The monoclinic angle β increases. It can be easily seen that the lattice parameters have the strongest pressure dependence with $\Delta a = 1.53$ Å, whereas b and c show a pressure dependence of $\Delta b = 0.76$ Å and $\Delta c = 0.93$ Å up to 27 GPa, respectively. The monoclinic angle increased by $\Delta\beta = 4.65^\circ$ in the same pressure region. The pressure dependence of the lattice constant a is almost twice as high as the change of the other two lattice constants b and c , which shows that the intermolecular bonding along the a -axis is softer and hence easily compressible than along other crystallographic axes. It can be argued that the behaviour of β is due to the reduction of the lattice parameters and the associated decrease of the layer distance. It is worthwhile to note that the decreases of the distances are smooth curves and hence the molecular motion becomes more localised at high pressures.

The molecular arrangement in crystal structure is mostly determined by molecular conformation and intermolecular interactions. In our work, the shortest intermolecular (π bonds) and interatomic (covalent bonds) distances as a function of pressure are showed in Figure 3. Comparing the pressure effect on the bond lengths and on the shortest intermolecular distances, we confirm the expected result that the intermolecular interactions

**Figure 2.** Pressure dependence of the lattice parameters a , b , c , and β of our work (the red line) compared to the literature data (Ref. [14]) (Online version in color).

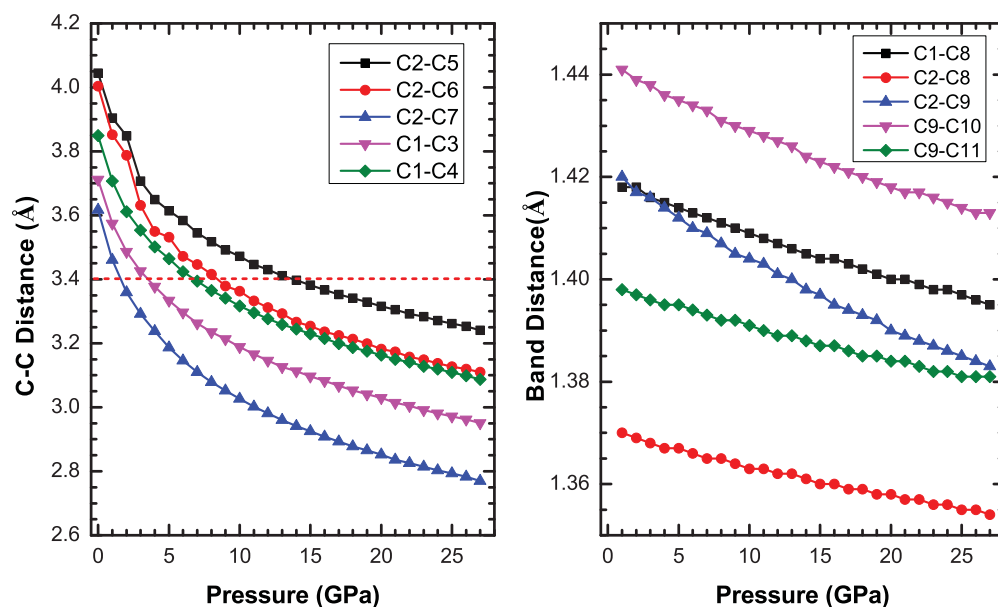


Figure 3. Pressure dependence of intermolecular carbon distances (the red dashed line marks the doubled van der Waals radius of a carbon atom [27]) (Online version in color).

are more sensitive to pressure than the intramolecular interaction. The dashed line marks the doubled vdW radius of a carbon atom (1.8 Å) at ambient pressure and temperature [27]. At ambient pressure, all the shortest intermolecular C–C and C–H distances are larger than this value. With increasing pressure, the decrease in C–C bond lengths turn out to be 1–16 mÅ between 0 and 27 GPa, but the shortest intermolecular C–C distances reduce 761 mÅ, respectively. It is remarkable that these distances decreased with increasing pressure smoothly. The layer distance decreases from 9.18 to 8.01 Å by 1.17 Å between ambient pressure and 27 GPa. The decreased interlayer distance leads to the increasing of the herringbone angle, implying that the two neighbouring molecules become more and more parallel. According to the results of this analysis, there is no evidence of structural phase transition up to 27 GPa. Such values naturally imply a large sensitivity of intermolecular interactions with pressure. However, the intermolecular interactions are anisotropically altered with pressure due to the non-uniform pressure dependence of the lattice parameters [12]. The difference in the changes is a reason for reorientation in the herringbone pattern where neighbouring molecules become more and more parallel.

With the knowledge of the lattice parameter under pressure, it is possible to give an equation of state (EOS) [28,29]. Figure 4 shows the unit cell volume V as a function of pressure in the parent compound anthracene at room temperature, where the red lines

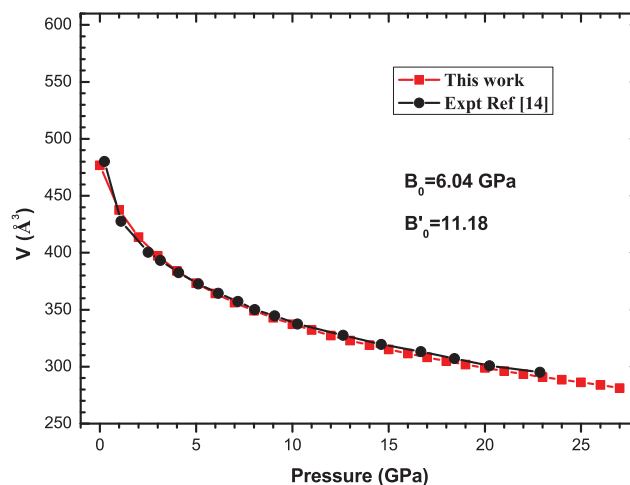


Figure 4. The unit cell volume compressibility of anthracene at room temperature. Experimental results as black dots are presented for comparison (Online version in color).

are the fitting results by using the third-order Birch–Murnaghan EOS, $P = \frac{3}{2} B_0 [(\frac{V}{V_0})^{-7/3} - (\frac{V}{V_0})^{-5/3}] \times \{1 + \frac{3}{4}(B'_0 - 4)[(\frac{V}{V_0})^{-2/3} - 1]\}$, where B_0 is the bulk modulus, B'_0 is the derivative of bulk modulus at ambient pressure, and V_0 is the volume at ambient pressure. Our calculations show that the volume decreases monotonically with pressure. With increasing pressure, we found that the calculated cell volume approaches the experimental values rather quickly. Up to 27 GPa, the volume compression is $V/V_0 = 58.9\%$. The bulk modulus at ambient pressure and temperature is

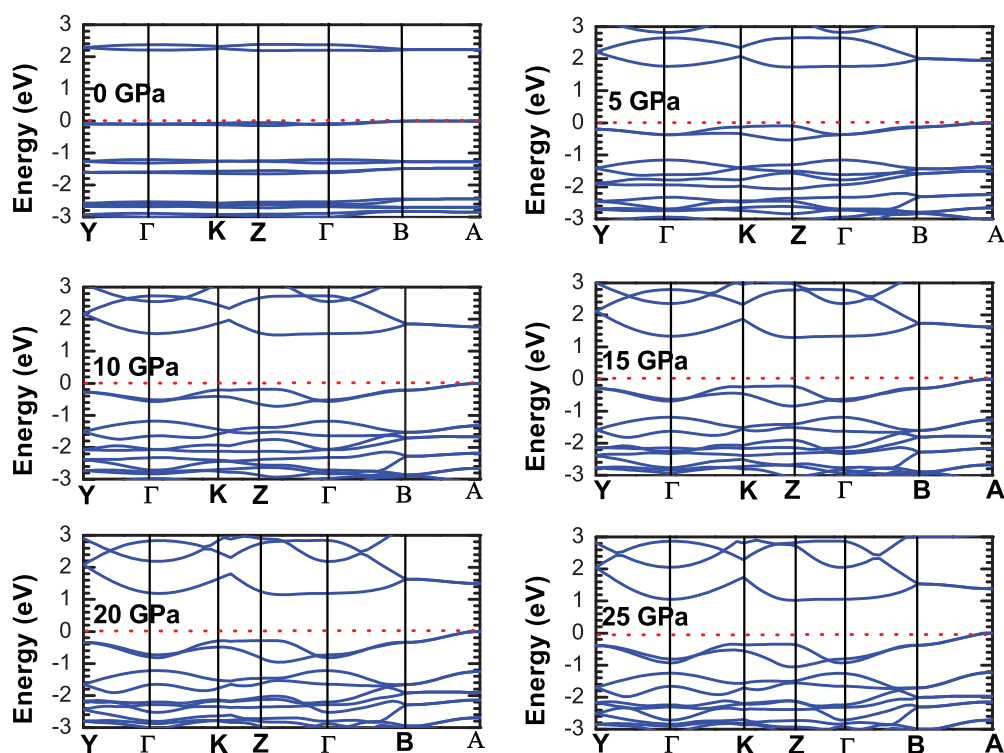


Figure 5. The dependence of the band gap of anthracene on pressure.

$B_0 = 5.94$ GPa and its derivative is $B'_0 = 12.38$. The experimentally reported values for $B_0 = 5.366 \pm 0.231$ and $B'_0 = 13.230 \pm 0.58$ [12]. Good agreement was achieved between the modelling and experiments. This result implies that the first-principles GGA simulation performed under high pressure might be more reliable due to the enhanced intermolecular interaction. As the unit cell volume is decreased, enhanced intermolecular interaction between neighbouring molecules increased. The increased intermolecular interaction also results in an enhanced band width of both valence and conduction bands, and therefore in a reduced band gap [30].

3.2. Band gap and electronic structure

Band gap is an important parameter to characterise the electronic structures of solids. Despite of this importance, very little experimental work is reported on the effect of pressure on the band gap of this semiconductor material. For this reason, a systematic study of the evolution of the band gap with pressure from 0 to 27 GPa has been carried out for anthracene. At ambient pressure, the band gap for solid anthracene is 2.2 eV at the GGA level, slightly higher than the LDA value (1.9 eV) [31]. The calculated band gaps of anthracene as functions of pressure are shown in Figure 5. One can see that the band gap reduces smoothly under compression without any significant discontinuity.

But in different pressure ranges, the average decrease of the band gap is different. When applying a linear fit in the lower and higher pressure range, respectively, the average decrease of the band gap up to 2 GPa is 0.07 eV/GPa and 0.05 eV/GPa from 2 to 10 GPa and 0.03 eV/GPa from 10 to 25 GPa. These data agree well with early theoretical results by Schatschneider et al. [17]. To determine the pressure coefficient, we fitted the direct band gap ($E_g(P)$)

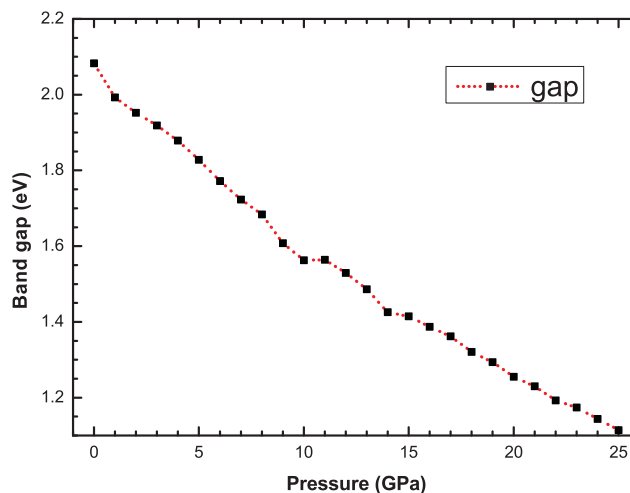


Figure 6. The band structures of anthracene at 0, 5, 10, 15, 20, and 25 GPa, respectively. The red dashed line is marked the Fermi level (Online version in color).

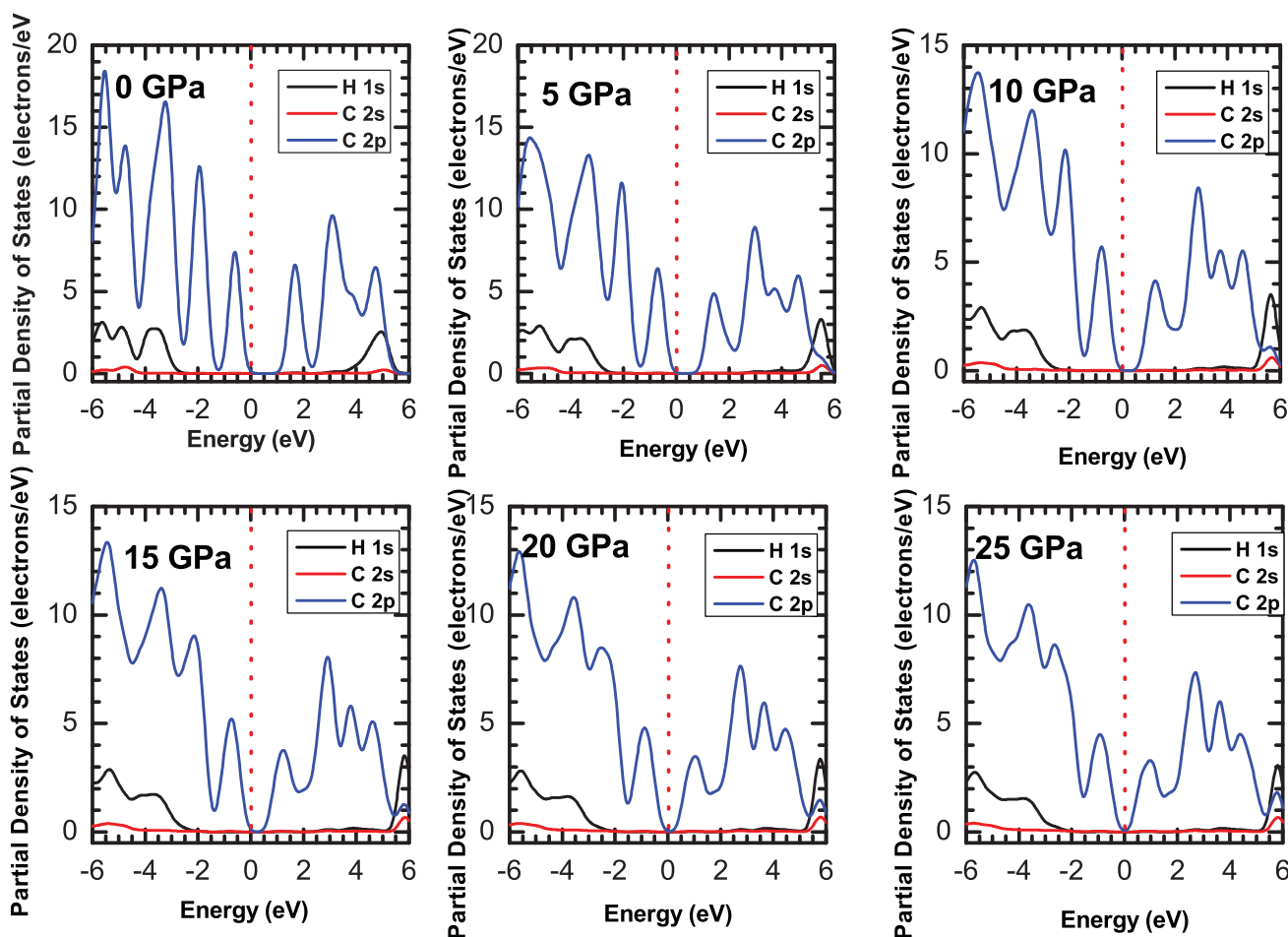


Figure 7. The partial density of state (PDOS) of anthracene at 0, 5, 10, 15, 20, and 25 GPa, respectively. The red dashed line is marked the Fermi level (Online version in color).

with a quadratic function, $E_g(P) = E_g(0) + aP + bP^2$, and obtained $a = -0.05$ eV/GPa and $b = 6.2$ eV/(GPa)².

The main features of the band structure of anthracene are anisotropic band dispersion and band splitting, which are three-dimensional effects and originate from the overlap of the π -wave functions of neighbouring molecules [13]. To further understand the origin of pressure dependence of the band dispersion and band splitting properties, we performed first-principle electronic structure calculations as a function of pressure. The band structures of anthracene at ambient pressure, 5, 10, 15, 20, and 25 GPa, are presented in Figure 6 as a representative example. It is seen that anthracene at high pressure is an indirect band gap semiconductor with the valence band maximum and conduction band minimum (CBM) at Z points. Since the crystal structure is layered, with a herringbone arrangement on the a - b plane, of molecules stacked along the c -axis, the electronic structure is more dispersive along the $2\pi/a - 2\pi/b$ axis. This is in accordance with the pressure dependence of the lattice parameter a , which is affected most by pressure. As the

pressure increases, the conduction and valence band shift to higher and lower energies, respectively. The shifts of the conduction and valence band result in a decreasing band gap. Thus, the anthracene is predicted to be an indirect band gap semiconductor, which is consistent with previous results from LDA [32].

Based on the partial density of state (PDOS), as presented in Figure 7, a slight shift of the peaks of DOS for conduction and valence bands are shifted to higher and lower range, and the reductions are consistent with the band structures. According to the PDOS, the valence and conduction bands near the Fermi level mainly come from C 2p and a strong hybridisation can be found between the H 1s state and the C 2p state in the conduction band energy between 4.96 and 5.47 eV. The CBM is mainly composed of H 1s and C 2p states. But the band energy between 5.4 and 6.1 eV mainly comes from H 1s. The valence band is derived from H 1s and C 2p states. The band energy between -6 and -1.1 eV mainly comes from C 2p, while H 1s contributes little in this energy range.

4. Conclusions

To extend our knowledge about the anthracene under high pressure, we used the DFT to study its structural and electronic properties. The variation of the structural quantities, such as cell parameters, volume, and interaction energy with increasing pressure does not show any discontinuity up to pressure 27 GPa. The calculated cell parameters and unit cell volume were compared with the experimental results reported by Oehzelt et al. and the agreement is very good over the entire pressure range. The pressure dependence of the electronic band structure, and band gap of anthracene were presented. The calculated electronic band splitting and the band gap reduce smoothly to some extent with the pressure increasing. Moreover, the pressure dependence of the electronic band structure, and the PDOS of anthracene were presented. This clearly indicates that the valence and conduction bands near the Fermi level mainly come from C 2p and a strong hybridisation can be found between the H 1s state and the C 2p state in the conduction band energy between 4.96 and 5.47 eV. The CBM is mainly composed of H 1s and C 2p states.

Acknowledgments

This work was supported by NSFC under grant nos. 11174284 and U1230202 (NSAF), the special Funds for Major State Basic Research Project of China (973) under grant no. 2012CB933702, and the Hefei Center for Physical Science and Technology under grant no. 2012FXZY004. The authors acknowledge National Supercomputing Center in Shenzhen for providing the computational resources and materials studio (version: 6.0; module:CASTEP).

Disclosure statement

No potential conflict of interest was reported by the authors.

Funding

This work was supported by NSFC [grant number 11174284], [grant number U1230202] (NSAF); the special Funds for Major State Basic Research Project of China (973) [grant number 2012CB933702]; the Hefei Center for Physical Science and Technology [grant number 2012FXZY004].

References

- [1] R. Mitsuhashi, Y. Suzuki, Y. Yamanari, H. Mitamura, T. Kambe, N. Ikeda, H. Okamoto, A. Fujiwara, M. Yamaji, N. Kawasaki, Y. Maniwa, and Y. Kubozono, *Nature* **464**, 76 (2010).
- [2] X.F. Wang, R.H. Liu, Z.Gui, Y.L. Xie, Y.J. Yan, J.J. Ying, X.G. Luo, and X.H. Chen, *Nat. Commun.* **2**, 507 (2011).
- [3] M. Xue, T. Cao, D. Wang, Y. Wu, H. Yang, X. Dong, J. He, F. Li, and G.F. Chen, *Sci. Rep.* **2**, 389 (2012).
- [4] H. Mitamura, X. Lee, X. He, Y. Yamanari, Y. Takahashi, Y. Suzuki, Y. Kaji, R. Eguchi, K. Akaike, and T. Kambe, *Phys. Chem. Chem. Phys.* **13**, 16476 (2011).
- [5] S. Tasch, C. Brandstaetter, F. Meghdadi, G. Leising, L. Athouel, and G. Froyer, *Adv. Mater.* **9**, 33 (1997).
- [6] R.B. Aust, W.H. Bentley, and H.G. Drickamer, *J. Chem. Phys.* **41**, 1856 (1964).
- [7] Q.W. Huang, G.H. Zhong, J. Zhang, X.M. Zhao, C. Zhang, H.Q. Lin, and X.J. Chen, *J. Chem. Phys.* **140**, 114301 (2014).
- [8] T. Kambe, X. He, Y. Takahashi, Y. Yamanari, K. Teranishi, H. Mitamura, S. Shibasaki, K. Tomita, R. Eguchi, H. Goto, Y. Takabayashi, T. Kato, A. Fujiwara, T. Kariyado, H. Aoki, and Y. Kubozono, *Phys. Rev. B* **86**, 214507 (2012).
- [9] C.P. Brock, and J.D. Dunitz, *Acta Crystallogr. Sect. B* **46**, 795 (1990).
- [10] J.R. Hemley, *Annu. Rev. Phys. Chem.* **51**, 763 (1989).
- [11] C.P. Brock and J.D. Dunitz, *Acta Crystallogr. B* **46**, 795 (1990).
- [12] M. Oehzelt and R. Resel, *Phys. Rev. B* **66**, 174104 (2002).
- [13] K. Hummer, P. Puschnig, and C. Ambrosch-Draxl, *Phys. Rev. B* **67**, 1841051 (2003).
- [14] M. Oehzelt, G. Heimel, and R. Resel, *J. Chem. Phys.* **119**, 1078 (2003).
- [15] Z.A. Dreger, H. Lucas, and Y.M. Gupta, *J. Phys. Chem. B* **107**, 9268 (2003).
- [16] R. Resel, M. Oehzelt, K. Shimizu, A. Nakayama, and K. Takemura, *Solid State Commun.* **129**, 103 (2004).
- [17] B. Schatschneider, S. Monaco, A. Tkatchenko, and J.J. Liang, *J. Phys. Chem. A* **117**, 8323 (2013).
- [18] B. Schatschneider, J.J. Liang, A.M. Reilly, N. Marom, G.X. Zhang, and A. Tkatchenko, *Phys. Rev. B* **87**, 060104 (2013).
- [19] L. Kronik and A. Tkatchenko, *Acc. Chem. Res.* **47**, 3208 (2014).
- [20] B. Schatschneider, S. Monaco, J.J. Liang, and A. Tkatchenko, *J. Phys. Chem. C* **118**, 19964 (2014).
- [21] A.M. Reilly and A. Tkatchenko, *J. Chem. Phys.* **139**, 024705 (2013).
- [22] K. Hummer, P. Puschnig, and C. Ambrosch-Draxl, *Phys. Rev. B* **67**, 184105 (2003).
- [23] M.D. Segall, P.J.D. Lindan, M.J. Probert, C.J. Pickard, P.J. Hasnip, S.J. Clark, and M.C. Payne, *J. Phys. Condens. Matter* **14**, 2717 (2002).
- [24] J.P. Perdew, K. Burke, and M. Ernzerhof, *Phys. Rev. Lett.* **77**, 3865 (1996).
- [25] A. Tkatchenko and M. Scheffler, *Phys. Rev. Lett.* **102**, 073005 (2009).
- [26] B.G. Pfrommer, M. Cote, S.G. Louie, and M.L. Cohen, *J. Comp. Phys.* **131**, 233 (1997).
- [27] A.I. Kitaigorodsky, *Molecular Crystals and Molecules* (Academic, New York, NY, 1973).
- [28] F. Birch, *J. Geophys. Res.* **57**, 227 (1952).
- [29] F. Birch, *J. Geophys. Res.* **91**, 4949 (1986).
- [30] K. Weinmeier, P. Puschnig, C. Ambrosch-Draxl, G. Heimel, E. Zojer, and R. Resel, *Mater. Res. Soc. Symp. Proc.* **665**, C8.20.1 (2001).
- [31] E.A. Silinsh, *Organic Molecular Crystals* (Springer-Verlag, Berlin, 1980).
- [32] A.S. Davydov, *Theory of Molecular Excitons* (Plenum Press, New York, NY, 1971).
- [33] R. Mason, *Acta Crystallogr.* **17**, 547 (1964).